



Transport times and anthropogenic carbon in the subpolar North Atlantic Ocean

Darryn W. Waugh^{a,*}, Thomas W.N. Haine^a, Timothy M. Hall^b

^a*Department of Earth and Planetary Sciences, Johns Hopkins University, 3400 N Charles St, Baltimore, MD 21218, USA*

^b*NASA Goddard Institute for Space Studies, New York, USA*

Received 25 July 2003; received in revised form 27 May 2004; accepted 24 June 2004

Available online 15 September 2004

Abstract

Simultaneous measurements of chlorofluorocarbons (CFCs), tritium, and helium are used to estimate the first two moments of the surface-to-interior transit times within the subpolar North Atlantic Ocean. The observed relationships among the different tracers implies that the transit-time distributions are broad, with width Δ approximately equal to the mean age T , indicating that mixing plays an important role in transport over decadal timescales. These broad transit-time distributions are further shown to be consistent with the observed time variations of mid-depth tritium in the Newfoundland Basin and Northeastern Atlantic between 1972 and 1997. We use the transit-time distributions inferred from the tracers to estimate the distribution, and change over the last two decades, of anthropogenic carbon in the subpolar North Atlantic. The values obtained are smaller than previous estimates using methods that have assumed weak mixing, with largest differences occurring in the Newfoundland Basin and Northeastern Atlantic. In the case of the uptake over the last two decades our estimate is 20–30% less than estimates that neglect mixing and use pCFC ages as water mass ages.

© 2004 Elsevier Ltd. All rights reserved.

Keywords: Tracers; Transit time distribution; Anthropogenic carbon; Labrador Sea Water; North Atlantic Ocean

1. Introduction

Deep convection and formation of large volumes of nearly homogeneous water occur within the subpolar North Atlantic Ocean, and these waters spread out into the North Atlantic and

beyond (e.g., Talley and McCartney, 1982), carrying high concentrations of dissolved oxygen, chlorofluorocarbons (CFCs), and anthropogenic carbon. Quantifying the timescales and pathways of this spreading is important for understanding not only ocean circulation but also regional and global climate.

Information on the spreading of these waters has been obtained from a variety of measurements,

*Corresponding author. Fax: +1-410-516-7933.

E-mail address: waugh@jhu.edu (D.W. Waugh).

including those of salinity and potential vorticity (e.g., Talley and McCartney, 1982), chemical tracers with time-varying sources or sinks (so called “transient tracers”) (e.g., Fine, 1995; Schlosser et al., 2001; Rhein et al., 2002), anomalies in hydrographic tracers (e.g., Sy et al., 1997; Curry et al., 1998; Koltermann et al., 1999), and subsurface floats (Lavender et al., 2000; Fischer and Schott, 2002). However, discrepancies exist between timescales derived from different tracers. For example, estimates of the spreading time of Labrador Sea Water (LSW) from the Labrador Sea to the Iceland and West European Basins vary from 4–5 yr from temperature and salinity anomalies (Sy et al., 1997) to greater than 10 yr from CFCs (e.g., Doney et al., 1997; Fine et al., 2002), while some subsurface floats make this transit in only 2 yr (Fischer and Schott, 2002).

A possible reason for these differences is that most studies have assumed weak mixing, so that a single timescale adequately summarizes the transport. However, in advective–diffusive flows, such as the oceans, there is not a single transit time but rather a distribution of transit times from one location to another (e.g., Beining and Roether, 1996; Deleersnijder et al., 2001; Haine and Hall, 2002; Khatiwala et al., 2001). Because of this distribution of transit times different tracer signals propagate at different rates (Waugh et al., 2003; Wunsch, 2002). This emphasizes the inherent complexity in interpreting tracer timescales, but also allows tracers of different time-dependencies to be used in combination to estimate transit-time distributions of a flow (Waugh et al., 2002, 2003).

Transit-time distributions (TTDs) provide a fundamental description of the transport in a flow. These distributions depend only on the transport and not the characteristics of any particular tracers. The characteristics of TTDs, in particular the breadth of the distributions, provide information of the relative roles of advection and “mixing”. Here mixing is used in a very general sense, and includes diapycnal mixing and isopycnal stirring by temporal and spatially varying eddies. Quantifying the TTDs in a flow is a complementary diagnostic to more traditional diagnostics of mixing, such as eddy diffusivities.

We use measurements of halocarbons (CFC11, CFC12, CFC113, and CCl_4), tritium, and helium-3 from several World Ocean Circulation Experiment (WOCE) cruises, between 1988 and 1997, to constrain the surface-to-interior TTDs in the subpolar North Atlantic Ocean. We examine the relationships among the different transient tracers, and show that the observed tracer–tracer relationships imply that the TTDs are broad. We also show that broad TTDs are consistent with the observed time variations of LSW tritium in Newfoundland Basin and Northeastern Atlantic between 1972 and 1997.

Given estimates of the TTDs it is possible to construct the interior concentration of conserved tracers from the tracer’s surface time series. An important application of this approach is estimating the distribution of anthropogenic carbon in the oceans (Thomas et al., 2001; Hall et al., 2002). In these calculations, the surface history of anthropogenic dissolved inorganic carbon (DIC_{ant}) is reconstructed from the history of atmospheric CO_2 and the equilibrium inorganic carbon system, and is then propagated into the ocean interior using the TTDs. We apply this method to the WOCE data to estimate the distribution of DIC_{ant} in the subpolar North Atlantic, as well as the change in concentration over the last two decades. We compare these to previous estimates that either (1) propagate the surface history into the interior using CFC ages as the water mass age (Thomas and Ittekkot, 2001; McNeil et al., 2003), or (2) uses Redfield ratios to account for biochemical sources and sinks (Gruber, 1998; Wanninkhof et al., 1999; Kortzinger et al., 1998, 1999; Gruber and Sarmiento, 2002). These previous methods all assume weak mixing. Our DIC_{ant} estimates using TTDs are in most instances smaller than previous estimates, with largest differences occurring in the Newfoundland Basin and Northeastern Atlantic.

2. Method

The approach used to constrain the transit time distributions (TTDs) is similar to that of Waugh et al. (2002, 2003). Measurements of transient tracers with different time dependencies are used to

determine the range of possible values of the first two moments of the TTDs. The basis of the approach is the fact that, for steady transport, the interior concentration $c(r, t)$ of a tracer with spatially uniform, time-varying surface concentration $c_0(t)$ is given by (Hall and Plumb, 1994; Haine and Hall, 2002)

$$c(r, t) = \int_0^{\infty} c_0(t - t') e^{-\lambda t'} G(r, t') dt', \quad (1)$$

where $G(r, t)$ is the TTD at location r and the $e^{-\lambda t'}$ term is for the radioactive decay of tracers with decay rate λ . Given interior concentration and surface time series of a particular tracer this relationship can be inverted to place constraints on G .

We assume, as in our previous studies, that the transport is steady and that the TTDs can be modeled as Inverse Gaussian functions (Chhikara and Folks, 1989; Seshadri, 1999), i.e.,

$$G(t) = \sqrt{\frac{\Gamma^3}{4\pi\Delta^2 t^3}} \exp\left(\frac{-\Gamma(t - \Gamma)^2}{4\Delta^2 t}\right), \quad (2)$$

where

$$\Gamma = \int_0^{\infty} \xi G(\xi) d\xi$$

is the mean transit time (“mean age”) and

$$\Delta^2 = \frac{1}{2} \int_0^{\infty} (\xi - \Gamma)^2 G(\xi) d\xi$$

defines the width Δ of the TTD. The impact of this assumption is discussed in Section 4.

With TTDs of the form (2), a given interior concentration (or age) of a transient tracer then limits Γ and Δ , for that location, to a range of values (see, e.g., Fig. 8 of Waugh et al., 2003). Measurement of the concentration (age) of a second tracer with sufficiently different time variations can further limit this range of values, and in some circumstances Γ and Δ can be tightly constrained.

To calculate tracer concentrations at interior locations using Eq. (1) it is necessary to know the surface time series of the tracers. For the halocarbons (CFCs, CCl_4) we use the atmospheric time series of Walker et al. (2000), solubility functions from Warner and Weiss (1985), Bu and

Warner (1995), and Hunter-Smith et al. (1983), and assume that all halocarbons are at 90% saturation in the surface waters. The largest uncertainty in determining the surface time series is the surface saturation (e.g., Haine and Richards, 1995). A wide range of surface saturations have been observed, and the saturation can vary between tracers, water masses, and years. We use a constant saturation primarily for simplicity. The sensitivity of our results to this assumption is discussed in Section 4 below. Note that CFC saturations much lower than 90% have been observed in newly formed LSW (e.g., Wallace and Lazier, 1988; Smethie et al., 2000). However, as we aim to determine the transit time distributions from the surface, rather than from the mid-depth locations of the newly formed water, it is more appropriate to use the saturation of surface water prior to convection. Rhein et al. (2002) and Pickart et al. (1996) used values of 85% and 100%, respectively, for saturation prior to cooling when modeling the formation of LSW.

The interior concentration of tritium is calculated using Eq. (1) with decay rate $\lambda = 0.05576 \text{ yr}^{-1}$ and a surface tritium time series based on that of Doney and Jenkins (1988). We have extended their time series to 1997 using the WOCE surface measurements. The sensitivity of our results to the assumed tritium time series is also discussed in Section 4 below. The interior concentration of excess helium (the component of helium-3 that has come from tritium decay) equals the concentration of tritium lost through radioactive decay.

In our analysis we convert CFC concentrations into pCFC ages, τ_{CFC} , defined as the elapsed time since the surface concentration was equal to the interior concentration. This conversion does not affect the determination of Γ and Δ , and the same results are obtained if CFC concentrations are used (as in Hall et al., 2002). However, the conversion into pCFC ages accounts for variations in the CFC distributions due to variations in the temperature and salinity, and means that CFC data with differing temperature and salinity can be easily compared. Although it is possible to calculate an age using tritium and excess helium together (e.g., Jenkins

and Clarke, 1976), we analyse each of these tracers separately.

3. Data

We use measurements from the WOCE A1, A2, and A16 lines (see Fig. 1). These lines pass through the Labrador and Irminger Seas, the Iceland, West European, and Newfoundland Basins, and the Rockall Trough, and the measurements sample a range of water masses including subpolar mode water, LSW, and Demark Strait and Iceland overflow waters. Measurements of CFC11, CFC12, tritium and helium-3 were made on all cruises analyzed here (along A1 in 1991 and 1994, along A2 in 1994 and 1997, and along A16 in 1988). CFC113 and CCl_4 were also measured on the two A2 cruises. The CFC, tritium, and helium-3 data (and the relationships among these tracers) from A16 has been examined by Doney et al. (1997), while Fleischmann et al. (2001) examined the CFC11 and tritium data from both cruises along A1 and the 1994 A2 cruise.

We also consider earlier measurements of tritium in the North Atlantic subpolar ocean.

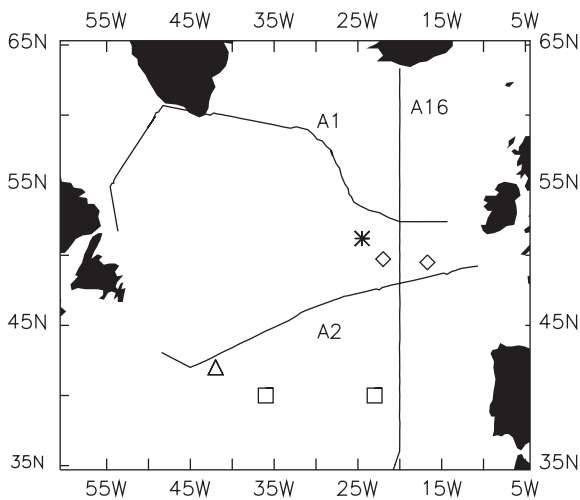


Fig. 1. Map of WOCE cruise lines A1, A2, and A16. Symbols show sites of additional tritium measurements from GEOSECS (triangle), CGFZ (asterisk), TTO (triangle, diamonds), and TOPOGULF (squares) studies used in Fig. 5.

Tritium measurements were made in the western part of the subpolar gyre in 1972 as part of the Geochemical Ocean Sections Study (GEOSECS) (Ostlund and Rooth, 1990). Repeat measurements at some of these sections and also in the eastern part of the gyre were made in 1981 as part of the Transient Tracers in the Ocean (TTO) study (Ostlund and Rooth, 1990). Measurements were also made in the subpolar North Atlantic in 1975 as part of a Charlie-Gibbs Fracture Zone (CGFZ) study (Top et al., 1987) and in 1986 as part of the TOPOGULF study (Andrie et al., 1988). We focus here on measurements made in the Newfoundland and West European Basins, near the WOCE A2 or A16 lines. In particular, GEOSECS station 27, CGFZ station 702, TTO stations 117, 118, and 228, and TOPOGULF stations 83 and 110, see Fig. 1.

4. Transit-time distributions

We first consider the relationships between tritium and CFC12 measurements. The symbols in Fig. 2 show the observed relationship between tritium and CFC12 age (τ_{CFC12}) for each of the five WOCE cruises. The relationships are remarkably similar among cruises, with the only significant difference being lower tritium for later years, consistent with the decay of tritium to helium. All data from the cruises are shown, but the relationships are still very compact: There is little dependence on basin (e.g., the 1994 A1 cruise samples the Labrador and Irminger seas as well as the Iceland Basin and the Rockall Trough) and a smooth transition with depth. The few points at young τ_{CFC12} with much higher tritium are for measurements in surface waters.

The curves in Fig. 2 show the modeled tracer relationships for TTDs with varying Γ and Δ . In Waugh et al. (2003) the modeled relationship between two tracer ages was presented for families of TTDs with fixed Γ and varying Δ (see Fig. 4 of Waugh et al., 2003). Here, however, we present the model relationships for families of TTDs with fixed Δ/Γ ratios: Each point on a curve in Fig. 2 corresponds to a particular value of Γ and Δ , with both values increasing for increasing τ_{CFC12} . This

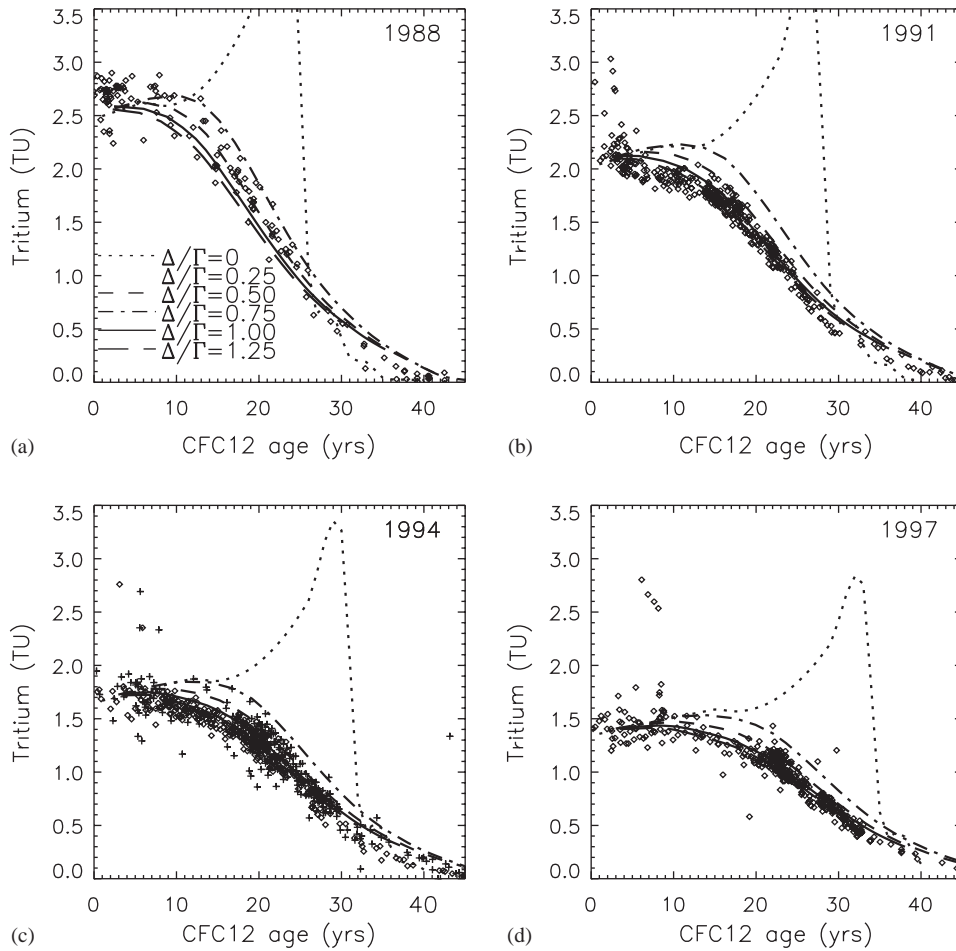


Fig. 2. Tritium concentration (TU) plotted against τ_{CFC12} for data from WOCE cruises in (a) 1988 (A16), (b) 1991 (A1), (c) 1994 (plus symbols for A1 and diamonds for A2), and (d) 1997, together with predictions from model TTDs (curves) with different Δ/Γ ratios.

choice of presentation was made because, as discussed below, model curves for fixed Δ/Γ can reproduce the observed tracer–tracer variations along a section.

Comparison of the modeled tritium– τ_{CFC12} relationships with the observations shows that small values of Δ/Γ , which correspond to a narrow TTDs and a steady, advectively dominated flow, are inconsistent with the observations for water masses with $\tau_{\text{CFC12}} > 10$ yr. For narrow TTD a large, well-defined, peak in the tritium is predicted for τ_{CFC12} between 20 and 30 yr (the time since the mid-1960s peak in the surface tritium), but such a peak is not observed. There is, however, good

model-data agreement for TTDs with $\Delta/\Gamma \geq 0.75$, with the model curves reproducing the observed variation of tritium with τ_{CFC12} , for all values of τ_{CFC12} . These large values of Δ/Γ correspond to broad TTDs, and hence a large range of transit times. For Δ/Γ larger than 1 there is very little difference in the modeled tritium– τ_{CFC12} relationships, and it is not possible to determine an upper limit of Δ/Γ from this analysis.

Although the above comparison cannot put any strong constraints on Δ/Γ for water masses with $\tau_{\text{CFC12}} < 10$ yr and only provides a lower limit for older water masses, it is remarkable that the model curves for fixed, large Δ/Γ can reproduce the

observed variation of tritium with τ_{CFC12} . This suggests that it may be appropriate to use a fixed value of Δ/Γ for an entire section. However, we cannot rule out the possibility of variable Δ/Γ , with, say, Δ/Γ increasing from around 0 for young τ_{CFC12} to much larger than 1 for old τ_{CFC12} .

If a fixed value of Δ/Γ is assumed for a complete section, then the values that best fit the observations varies among the different WOCE lines, see Table 1. However, the differences between Δ/Γ from different lines are probably not significant given that larger differences result from varying the boundary conditions within uncertainties, see Table 1 and discussion below. Also, there is no systematic variation in estimated Δ/Γ with measurement date, and the repeat measurements along A1 and A2 yield similar values. This result is consistent with, although does not imply that, relatively small time variations in the transport during the measurement period.

Although the CFC12 surface history is well known, the degree of saturation in surface waters is uncertain. There is also uncertainty in the surface history of tritium, especially during the 1960s and 1970s. In the calculations presented we have assumed a saturation of 90% for CFC12 and used a tritium surface history based on that of Doney and Jenkins (1988). We have repeated the above analysis using different CFC saturations and tritium time series (as in Doney and Jenkins (1988) we use an uncertainty of 5% for the surface tritium time series). The Δ/Γ that best fits the tritium– τ_{CFC12} observations for several different surface conditions are listed in Table 1 (again, when determining Δ/Γ we assumed a fixed value

for the whole section). The best-fit Δ/Γ varies with CFC saturation and surface tritium but in general remains around or larger than 1, and the variation with changing the surface time series is similar to the variation between WOCE lines. Because of these uncertainties (and also the assumption of a particular form of the TTDs, see discussion below) it is not possible to determine a precise value of Δ/Γ . However, the general conclusion that the TTDs are broad and there is a wide range of transit times still holds.

The relationships among the other transient tracers measured also place constraints on Δ/Γ , and can be used to test the above inferences from tritium and CFC12. Fig. 3 compares the observed and modeled relationships of the other transient tracers with τ_{CFC12} for measurements made along A2 in 1997 (very similar relationships hold for the other cruises). The ages from the measurements of CFC11, CFC113, and CCl_4 are, in general, different from those from CFC12. This is expected for flows with mixing because of the different temporal histories of the tracers (Waugh et al., 2003).

For young water masses the observed τ_{CFC11} is older than τ_{CFC12} , whereas the reverse is true for ages older than 25 yr. These differences are consistent with broad TTDs with $\Delta/\Gamma \geq 0.5$, but not for $\Delta/\Gamma \leq 0.25$. Thus, in contrast with the tritium– τ_{CFC12} analysis, the $\tau_{\text{CFC11}}-\tau_{\text{CFC12}}$ relationship indicates a lower limit of Δ/Γ (≥ 0.5) for young water masses. Note that even for very broad TTDs the modeled differences in CFC ages is less than observed for young water masses. This difference is removed if a slightly higher surface

Table 1

Best fit Δ/Γ for different WOCE cruises, and different CFC12 saturations (ξ) and surface tritium time series

Line	Year	Standard	$\xi = 1.0$	$\xi = 0.8$	${}^3\text{H} \times 1.05$	${}^3\text{H} \times 0.95$
A16	1988	0.80	0.65	1.05	1.00	0.65
A1	1991	1.25	0.95	1.75	1.80	0.95
A1	1994	1.35	1.05	1.80	1.90	1.05
A2	1994	1.10	0.95	1.55	1.50	0.85
A2	1997	1.10	0.85	1.45	1.35	0.85

The “standard” calculation used $\xi = 0.9$ and tritium time series based on that of Doney and Jenkins (1988). Results in $\xi = 1.0$ and 0.8 columns used these CFC saturations and the standard tritium time series, whereas results in the ${}^3\text{H} \times 1.05$ and ${}^3\text{H} \times 0.95$ columns used $\xi = 0.9$ but tritium time series modified by 5%.

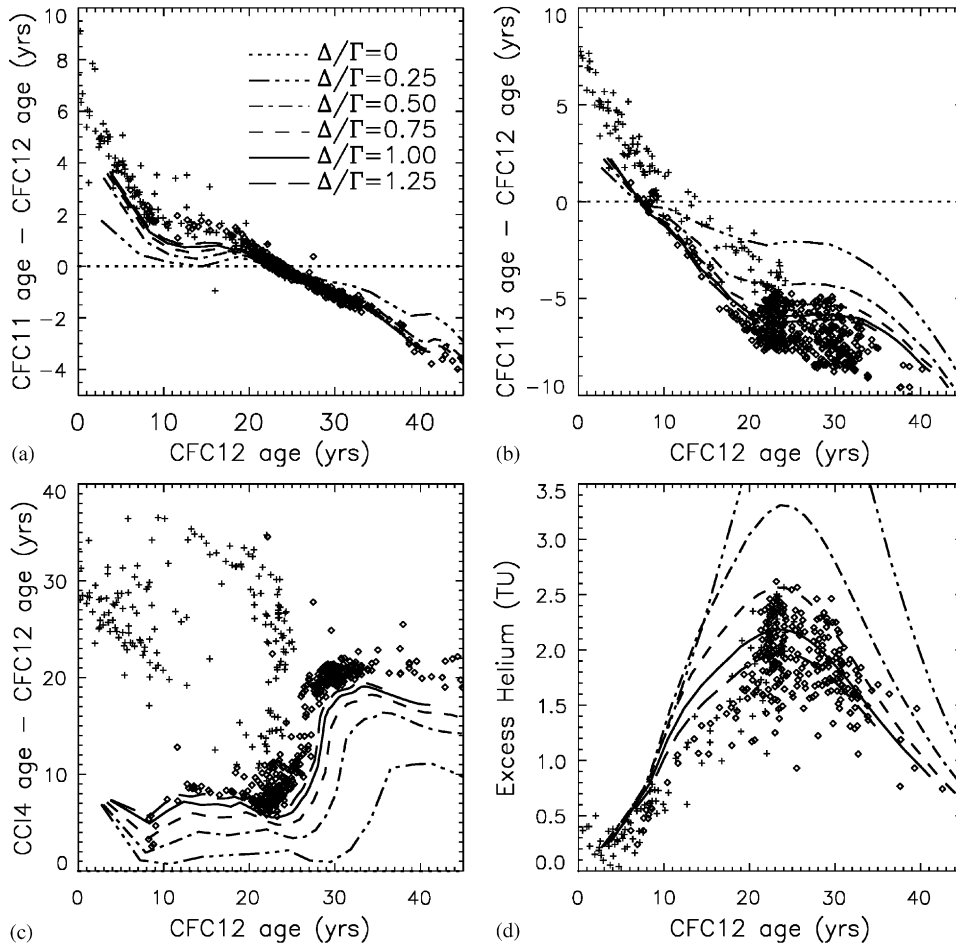


Fig. 3. Relationships between (a) $\tau_{\text{CFC11}} - \tau_{\text{CFC12}}$, (b) $\tau_{\text{CFC113}} - \tau_{\text{CFC12}}$, (c) $\tau_{\text{CCl4}} - \tau_{\text{CFC12}}$, and (d) excess helium, with τ_{CFC12} for measurements along A2 in 1997 (symbols) and for model TTDs (curves). Plus symbols in panels (b) and (c) correspond to observations in water with temperatures warmer than 5°C .

saturation, of around 2%, is used for CFC12 than for CFC11 (this applies for CFC12 saturations between 80% and 100%).

There is more scatter in the observed relationships for τ_{CFC113} and τ_{CCl4} with τ_{CFC12} . The majority of this scatter is for measurements in warm waters ($T > 5^\circ\text{C}$), and for these waters the observed τ_{CFC113} and τ_{CCl4} are older than modeled even for very large Δ/Γ . These differences are consistent with the biochemical degradation of these tracers in warm waters (e.g., Roether et al., 2001; Wallace et al., 1994; Huhn et al., 2001). Biochemical loss results in lower concentrations which, if not accounted for, appear as older ages.

If only waters colder than 5°C are considered then the observed variations of τ_{CFC113} and τ_{CCl4} with τ_{CFC12} indicate that $\Delta/\Gamma > 0.75$, consistent with the above analysis.

Even for cold waters the modeled τ_{CCl4} for Δ/Γ much larger than 1 is less than observed. One explanation of this is lower surface saturation of CCl4 : Modeled τ_{CCl4} for $\Delta \approx \Gamma$ matches the data in cold waters if a CCl4 saturation of 80% is used with a CFC12 saturation of 90%. Another explanation is a slower CCl4 loss in cold waters. If we assume that the loss is a first-order process with loss rate λ (i.e., the loss equals a constant λ times the concentration) we can obtain an estimate

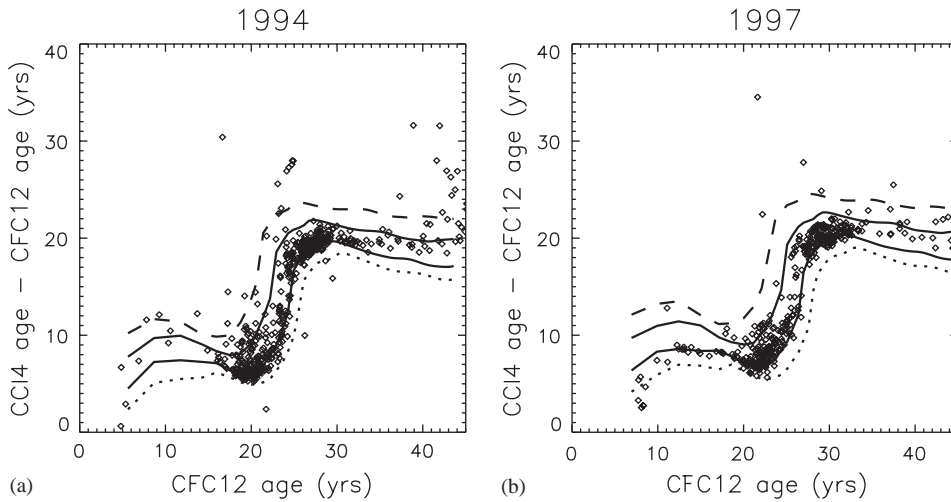


Fig. 4. Relationships between τ_{CCI4} and τ_{CFC12} for measurements (in waters colder than 5°C) along line A2 (symbols) and for model TTDs (curves), for (a) 1994 and (b) 1997. The different curves correspond to λ equal to 0 (dotted), 0.005 yr^{-1} (lower solid), 0.015 yr^{-1} (upper solid), and 0.025 yr^{-1} (dotted). $\Delta = \Gamma$ in all calculations.

of λ by using the TTDs implied by other tracers (e.g., tritium and CFC12) in Eq. (1) and determining the λ that reproduces the observed $\tau_{\text{CCI4}}:\tau_{\text{CFC12}}$ relationships. Fig. 4 shows the observed $\tau_{\text{CCI4}}:\tau_{\text{CFC12}}$ relationships (for $T < 5^\circ\text{C}$) from the two A2 cruises together with model curves for TTDs with $\Delta = \Gamma$ for varying λ (a saturation of 90% is used for both tracers). There is some scatter and λ can only be constrained to a range of values, i.e., the observations generally fall within curves for $\lambda = 0.005$ and 0.015 yr^{-1} . Repeating these calculations assuming TTDs with Δ/Γ equal to 0.75 or 1.25 produces very similar results. This loss rate is higher than the values of less than 0.1% per year determined by Huhn et al. (2001) (from measurements in the South Atlantic), but still represents very slow loss. Also, using a lower CCI_4 saturation in our calculations would result in lower values for the loss rate (as mentioned above, a saturation of 80% would imply no loss). Repeating this analysis for slightly warmer waters yields larger loss rates: For temperatures between 5 and 7.5°C the loss is around 3% per year, while for temperatures between 7.5 and 10°C the loss is around 8% per year (not shown). Hence, as in Huhn et al. (2001), our analysis indicates that the loss rate increases very rapidly with temperature.

The observed relationship between excess helium and τ_{CFC12} also implies broad TTDs with $\Delta \approx \Gamma$ (Fig. 4d). In contrast to the other tracer–tracer relationships, the modeled relationship between excess helium and τ_{CFC12} is sensitive to Δ/Γ for large values. This suggests that the observed relationship may constrain the TTD more tightly than the other tracer pairs. Unfortunately there is a lot of scatter in the data, and it is not possible to determine precise values of Δ/Γ . The excess helium in young waters is less than modeled even for very large Δ/Γ . This may be due to rapid loss of helium within the mixed layer to the atmosphere. In contrast, the excess helium in old water masses tends to be higher than modeled for $\Delta/\Gamma \approx 1$. This is likely due to primordial helium, which is not accounted for when calculating excess helium. The cause of the increased scatter for intermediate ages is unclear, and may be due to uncertainties in the calculation of excess helium.

The excess helium–tritium relationship (not shown) has a similar “hook” shape as the above excess helium– τ_{CFC12} relationship, and is also reasonably well modeled by TTDs with $\Delta \approx \Gamma$. Similar excess helium–tritium distributions have been reported by Jenkins (1988) for TTO data, Andrie et al. (1988) for their 1983 data and Doney

et al. (1997) for the A16 data. Jenkins (1988) noted that peak tritium values were much lower than expected for advective flow, and further showed that a one-dimensional model with Peclet number around 1 best matches the TTO data. This is consistent with our above analysis as $\Delta/\Gamma = 1$ corresponds to a Peclet number of 1 for one-dimensional flow with uniform advection and diffusion (Waugh and Hall, 2002).

As a final check on the above estimates of Γ and Δ we now examine the temporal variation of tritium. Tritium measurements have been made in the Newfoundland and West European basins several times since 1972 (see Section 3 and Fig. 1), and these can be used to test whether the temporal variation is consistent with broad TTDs. Although the location of these measurements varies (see Fig. 1) the measurements of LSW along A2 and A16 suggest that these locations have similar tritium and CFC-12 concentrations in LSW (i.e., there are only small variations in LSW tracer concentrations along A2 between 45 and 20 W and along A16 between 40 and 50 N). The symbols and vertical bars in Fig. 5 show the evolution of tritium for the measurements between 1972 and 1997, at

the locations shown in Fig. 1. The symbols correspond to values around 1500 m, and the vertical bars show the upper and lower limits of values between 1200 and 1800 m. There is a difference in the vertical gradients of tritium between the early and late measurements: Measurements before 1988 show large vertical gradients around 1500 m, whereas those in 1988 and later show very weak vertical gradients. In addition, the values before 1988 are based on only one or two profiles for each year, and these early profiles have much lower vertical resolution than WOCE measurements. This means there is larger uncertainty in the LSW tritium in the 1970s and early 1980s.

Also shown in Fig. 5 is the predicted evolution of tritium for several different TTDs. Again we assume the TTDs do not change with time and that the TTDs are of form (2). The TTDs have different values of Δ/Γ , and the value of Γ and Δ are chosen so that the modeled tritium in 1994 is the same. Comparison with the observations shows that the observations are inconsistent with narrow TTDs ($\Delta/\Gamma \leq 0.5$). We draw the same conclusion even if we only use observations during and after 1988, for which there are numerous measurements in LSW for each year and well defined tritium values. The tritium data from the 1970s also indicate that very broad TTDs, with $\Delta/\Gamma > 1.5$, are unrealistic. So the tritium observations indicate that $0.5 < \Delta/\Gamma < 1.5$ for LSW. Because of the dearth of measurements and large vertical gradients in the 1970s and early 1980s, and uncertainty in the tritium surface time series, it is not possible to place a tighter constraint on Δ/Γ or to examine possible time variations in the transport and TTDs.

The above analysis shows that steady transport with TTDs with $\Delta \approx \Gamma$ can reproduce not only the tracer–tracer relationships observed between 1988 and 1997 but also the observed change in LSW tritium between 1972 and 1997. As mentioned above, TTDs with $\Delta \approx \Gamma$ are very broad and correspond to a large range of transit times. This is illustrated in Fig. 6(a) where the TTDs with $\Delta = \Gamma$ and τ_{CFC12} (in 1994) = 10, 15, 20, and 25 yr are shown. These TTDs are asymmetric, have narrow peaks at transit times younger than the CFC age

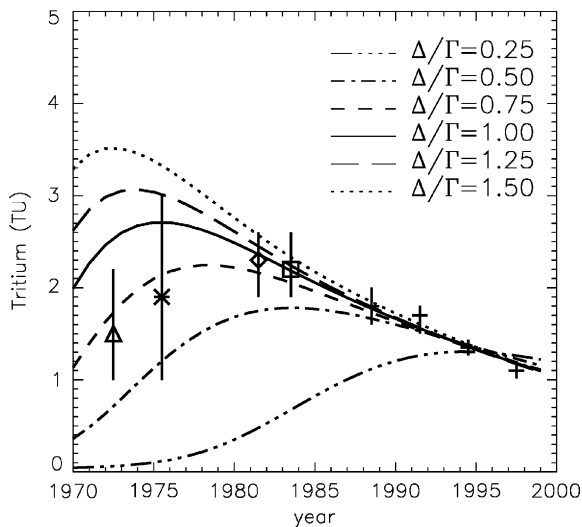


Fig. 5. Observed time variation of LSW tritium (symbols plus vertical lines) in the Newfoundland and West European Basins (see text and Fig. 1) and predictions for TTDs with different Δ/Γ (curves). Values of Γ and Δ are chosen, for each Δ/Γ , so that tritium in 1994 is the same.

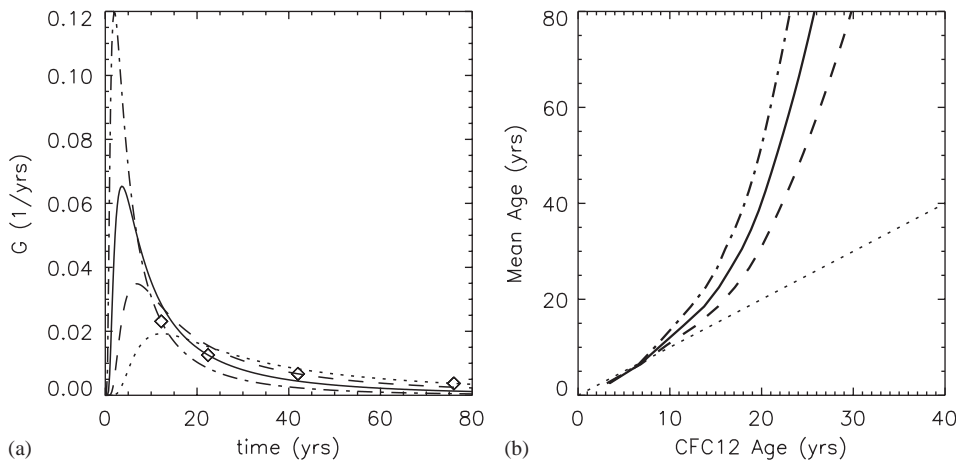


Fig. 6. (a) TTDs with $\Delta = \Gamma$ that produce (in 1994) τ_{CFC12} equal to 10 (dot-dashed curve), 15 (solid), 20 (dashed), and 25 (dotted) yr. Symbols show Γ for each TTD. (b) Variation of Γ with τ_{CFC12} (in 1994) for TTDs with Δ/Γ equal to 0 (dotted), 0.75 (dashed), 1.0 (solid), and 1.25 (dot-dashed).

(the mode time varies from 2 to 12 yr), and have long tails representing old water components. Importantly, the mean Γ (symbols) is much larger than the CFC12 ages. The difference between Γ and τ_{CFC12} for TTDs with different Δ/Γ is shown in Fig. 6(b). There are large differences for CFC12 ages greater than 15 yr. This shows that for much of the subpolar gyre CFC12 ages are much younger than the mean transit time.

A source of uncertainty in our analysis arises from the use of a particular functional form for the TTD, in this case the Inverse Gaussian form. It is unlikely that the real TTDs resemble Inverse Gaussian distributions. The present results suggest that the real TTDs have Δ/Γ around 1 and are skewed, but they exert no further constraints. Waugh et al. (2002, 2003) examined the sensitivity to the shape of the TTD, looking at the impact of bimodality on tracers. They found that, for tracers whose history spans the TTD, once the first and second moments (Γ and Δ) are determined, there is little additional sensitivity to higher moments. In fact, to the extent a tracer's surface history can be modeled as a quadratic function in time, only the first two moments of the TTD affect its concentration (Waugh et al., 2003). On the other hand, the TTD at transit times older than the history of the tracers cannot be constrained by the tracers.

Thus, for example, one cannot rule out, on the basis of the above transient tracers alone, a second peak in the TTD at transit times beyond 40–50 years. (Because of its longer atmospheric history τ_{CCl4} may provide some information, but its slow oceanic loss complicates interpretation of the measurements.) If a second, very old peak exists our finding regarding Δ/Γ may be too low. However, it seems unlikely that such a long transit time dominates transport in the subpolar north Atlantic.

5. Anthropogenic carbon

An important application of transient tracers is the estimation of anthropogenic carbon distribution and uptake. The fact that there is a wide range of transit times due to mixing needs to be considered in this application. Several different methods to infer anthropogenic carbon have been developed, and there are considerable discrepancies among the estimates (e.g., Wallace, 2001; Wanninkhof et al., 1999). Most methods assume mixing to be weak, which, in light of our tracer analysis, appears to be erroneous for much (if not all) of the subpolar North Atlantic. A new method has been proposed by Hall et al. (2002) that does

not assume mixing to be weak, and, in addition, does not require the use of uncertain Redfield ratios to account for biochemical sources and sinks of carbon (see also Thomas et al., 2001). In this method, TTDs inferred from tracers are used to propagate to the interior an estimate of the surface history of DIC_{ant} .

As in most other studies, the surface DIC_{ant} history is calculated from equilibrium inorganic carbon chemistry by assuming the air-sea CO_2 disequilibrium to be constant in time (but not necessarily zero). In the calculations below we use $DIC_{ant}(t) = DIC(t) - DIC(1780)$, where $DIC(t)$ is the dissolved inorganic carbon at time t and the year 1780 is used as the start of the preindustrial

era to be consistent with previous studies that assumed a preindustrial atmospheric CO_2 concentration of 280 ppm. We do not assume that the disequilibrium term is spatially uniform: As in Gruber et al. (1996), we assume that the disequilibrium term is dominated by its preindustrial value, which varies from outcrop to outcrop.

We calculate DIC_{ant} along A1 and A2 using the TTDs inferred from the CFC12 measurements in 1994 assuming a fixed Δ/Γ for all data. Given a value of Δ/Γ , a CFC12 measurement enables values of Γ and Δ to be uniquely determined (see Section 4), and then DIC_{ant} to be calculated. Fig. 7 shows the average vertical profiles DIC_{ant} , in 1993, for (a) Irminger Sea, (b) Iceland Basin, (c) Newfoundland Basin, (d) West European Basin, calculated from CFC12 data and TTDs with different values of Δ/Γ . $\Delta = 0$. Horizontal lines in (d) are the range of previous estimates for this region.

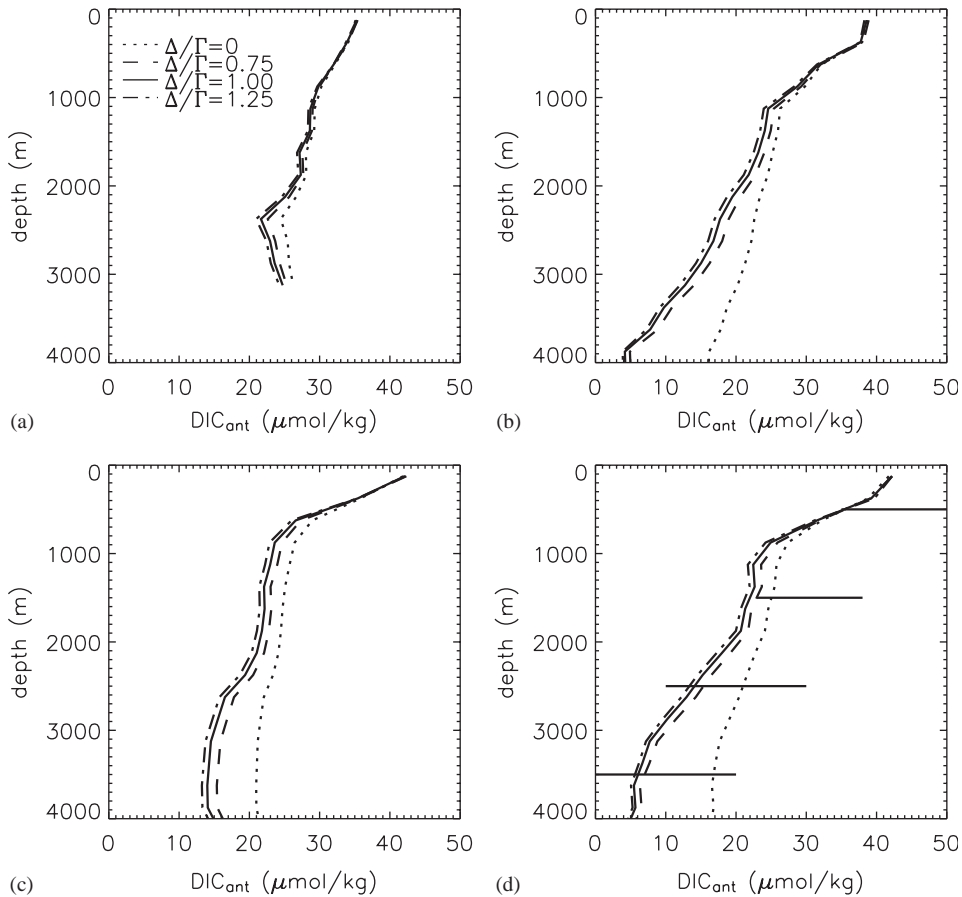


Fig. 7. Average vertical variation of DIC_{ant} in 1993 for (a) Irminger Sea, (b) Iceland Basin, (c) Newfoundland Basin, (d) West European Basin, calculated from CFC12 data and TTDs with different values of Δ/Γ . $\Delta = 0$. Horizontal lines in (d) are the range of previous estimates for this region.

(c) Newfoundland Basin, and (d) West European Basin, for several different Δ/Γ . (As we assume the TTDs do not change with time we can calculate DIC_{ant} for any year, and values for 1993 are shown here to enable comparison with other estimates, see below.) There is only weak sensitivity of DIC_{ant} to the exact value of Δ/Γ for values within the range constrained by the transient tracers (i.e., $\Delta/\Gamma \geq 0.75$), with the difference in DIC_{ant} generally between 0.5 and 1.5 $\mu\text{mol}/\text{kg}$. Using even larger Δ/Γ results in virtually no change in DIC_{ant} . Thus, the inability of the tracer analysis to provide an upper bound on Δ/Γ has little impact on the DIC_{ant} estimation.

There is, however, a large difference between the values obtained using realistic values of Δ/Γ and those obtained assuming $\Delta = 0$, for mid- and lower depths ($\tau_{\text{CFC12}} > 10 \text{ yr}$). This difference is because the CFC12 history is, generally, more non-linear than DIC_{ant} , and, therefore, CFC12 ages preferentially weight young components of broad TTDs, compared to DIC_{ant} . One then looks too recently in the DIC_{ant} surface history, causing overestimates in DIC_{ant} (Hall et al., 2002; Waugh et al., 2003). This overestimate increases with CFC age, and the difference between calculations of DIC_{ant} using realistic Δ/Γ and those assuming $\Delta = 0$ is largest in the eastern part of the subpolar ocean where the ages are largest. For example, the column DIC_{ant} from $\Delta = 0$ calculations is 5%, 30%, 25%, and 40% larger than from $\Delta = \Gamma$ calculations for the Irminger Sea, Iceland Basin, Newfoundland Basin, and West European Basins, respectively.

The distribution of DIC_{ant} shown in Fig. 7 is qualitatively similar to previous estimates (e.g., Kortzinger et al., 1998; Thomas and Ittekkot, 2001). DIC_{ant} has penetrated throughout the water column in all basins, and the concentration decreases with depth and from west to east consistent with the increase in “age” of the water masses. An exception to the increase with depth occurs in the Irminger Sea where there is an increase at the bottom due to the presence of “young” Demark Strait overflow water.

Although there is qualitative agreement with previous estimates there are significant quantita-

tive differences. For example, the horizontal lines in Fig. 7d show the ranges from several contemporaneous DIC_{ant} estimates for the same location and time (Wanninkhof et al., 1999; Kortzinger et al., 1998, 1999; Gruber and Sarmiento, 2002), which use either the Gruber et al. (1996) or Chen and Millero (1979) methods. (It is important to note the range in the previous DIC_{ant} estimates is not solely due to the different methods, and studies that ostensibly apply the same method to the same data obtain different estimates.) Our estimates are lower than previous estimates in upper and middle levels, and within the range of other estimates for deep waters. Comparisons of our calculations with estimates of 1982 DIC_{ant} concentrations by Gruber (1998), in both the eastern and western basins of the subpolar gyre, show differences consistent with these biases: Our estimates are lower in upper waters but similar or larger in deeper waters.

Some of the differences between our estimates and those from calculations using the Gruber method can be explained by biases in the treatment of transport. In upper and middle (“fully contaminated”) isopycnals the tracer ages are used as the water mass age in the Gruber method to estimate the disequilibrium term. This neglect of mixing causes a high bias in the disequilibrium term, and hence in DIC_{ant} . On the other hand, in deep (“uncontaminated”) isopycnals the measured DIC is assumed to be the preindustrial value. If mixing brings in small, non-zero concentrations of DIC_{ant} on these isopycnals then the Gruber method overestimates the preindustrial DIC, and hence underestimates DIC_{ant} . See Hall et al. (2002) for further discussion.

Our estimate in upper waters (e.g., 500 m) is at the lower end of the range of previous estimates. The differences here are not due to the different treatment of the transport in our and previous methods as DIC_{ant} is not sensitive to Δ/Γ at this depth (see Fig. 7). Also our calculation of CFC ages is consistent with the previous studies, and we make the same assumption of constant disequilibrium. A possible cause of the differences is uncertainties in the other inference techniques, e.g., uncertainties in Redfield ratios (Wanninkhof et al., 1999). In fact, Wanninkhof et al. (1999) and

Gruber and Sarmiento (2002) apply the Gruber method to the same data but obtain very different estimates in the upper waters: Wanninkhof et al. (1999) obtain a value around $35 \mu\text{mol/kg}$ for DIC_{ant} at 500 m whereas Gruber and Sarmiento (2002) obtain a value around $50 \mu\text{mol/kg}$.

Accounting for mixing is also important for calculations of the change in DIC_{ant} over a certain period. McNeil et al. (2003) have recently calculated the DIC_{ant} uptake between 1980 and 1999 using CFC ages as the water mass age, which is equivalent to our $\Delta = 0$ calculation. However, as shown in Fig. 8 the values calculated using $\Delta = 0$ are significantly larger than calculations assuming realistic values of Δ/Γ . Note there is a difference in the change in DIC_{ant} in the upper waters even though there is no difference in the 1993 DIC_{ant}

shown in Fig. 7. This is because the impact of the assumption of no mixing on estimates of DIC_{ant} from CFC ages varies with time. In 1980 DIC_{ant} in young waters is slightly underestimated if no mixing is assumed, whereas in 1990 assuming no mixing results in a slight overestimate of DIC_{ant} for the same waters. The net result is a noticeable overestimate in the change in DIC_{ant} between 1980 and 1999. In terms of the column uptake of DIC_{ant} , assuming no mixing results in an overestimate (compared to calculations using $\Delta/\Gamma = 1$) of 15% in the Irminger Sea, 25% in the Iceland Basin, and greater than 30% in the Newfoundland and West European Basins. We conclude that the McNeil et al. (2003) “no mixing” calculations of DIC_{ant} uptake in the subpolar North Atlantic Ocean are a significant overestimate.

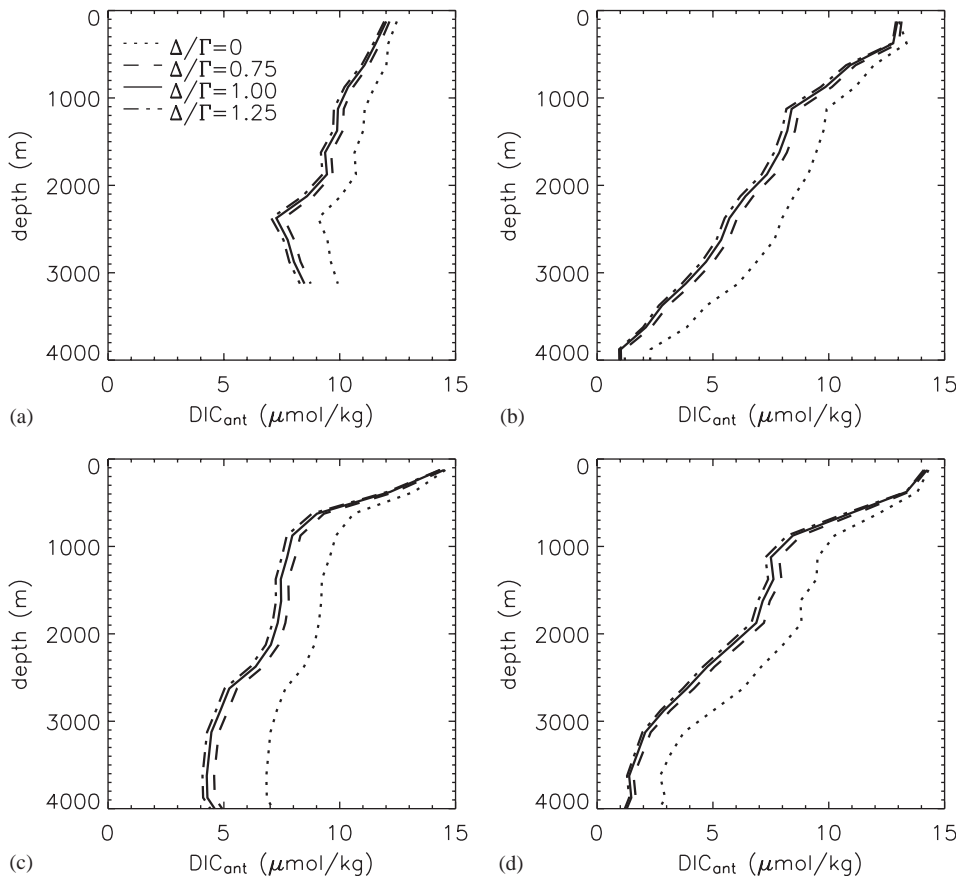


Fig. 8. As in Fig. 7 except for uptake of DIC_{ant} between 1980 and 1999.

Hall et al. (2004) recently applied a modified, inventory-based TTD method to Indian Ocean CFC data, and found a significant difference between weak and strong mixing calculations of the decadal-scale DIC uptake. Consistent with our results, their uptake estimate in the weak-mixing limit was about 30% larger than the strong-mixing limit.

There are several uncertainties in our estimates of DIC_{ant} (and change in DIC_{ant}). There is uncertainty in Δ/Γ . However, as discussed above, this results in a relatively small uncertainty in DIC_{ant} ($\pm 1 \mu\text{mol/kg}$). There is also uncertainty in the surface saturation of CFC12 used in the CFC age calculation. Using a smaller saturation results in a smaller CFC age and hence a larger DIC_{ant} (and the reverse for a larger saturation). However, when a smaller (larger) saturation is used the best-fit Δ/Γ is larger (smaller), see Table 1. The change in DIC_{ant} due to this change in Δ/Γ is in the opposite sense of that due to the change in CFC age, and the net result of these two compensating changes is small. For example, if the CFC saturation is varied by 10% the change in DIC_{ant} is of similar magnitude to changes in Δ/Γ (generally less than $2 \mu\text{mol/kg}$). Thus, the uncertainty in our estimates of column total DIC_{ant} due to uncertainties in characterizing the TTDs is around 5–10%, which is much less than the difference between our estimates and the previous estimates discussed above.

Another source of uncertainty in our DIC_{ant} estimates is the uncertainty in the surface DIC_{ant} time series. In particular the uncertainty is due to the assumption of constant disequilibrium. Hall et al. (2004) relaxed the constant-disequilibrium assumption in their analysis of the Indian Ocean, and estimated a reduction of 6–9% in DIC_{ant} . Their method to allow time-varying disequilibrium requires knowledge of DIC_{ant} over entire volumes bounded by isopycnals, and cannot be applied to the calculations here on specific WOCE lines. However their analysis showed that allowing variable disequilibrium always acts to reduce DIC_{ant} estimates, and so our estimates, already lower than previous estimates, most likely represent upper bounds on DIC_{ant} .

6. Concluding remarks

Measurements of transient tracers in the sub-polar North Atlantic Ocean place tight constraints on the first two moments of the surface-to-interior transit time distributions (TTDs). The relationships among chlorofluorocarbons (CFCs), tritium, and helium from five cruises (between 1988 and 1997) and the temporal variation of tritium in LSW between 1972 and 1997 all indicate that the TTDs are very broad, with width Δ approximately equal to the mean Γ (see Table 1 for range of estimates). Furthermore, the main features of the observed tracer–tracer relationships and the temporal evolution of tritium can be reproduced assuming steady transport with Inverse Gaussian TTDs with $\Delta = \Gamma$.

The existence of broad TTDs is consistent with subsurface floats that show strong internal recirculations, with a few floats making rapid transits across the subpolar gyre but the majority remaining in western or eastern part of the gyre (e.g., Lavender et al., 2000; Bower et al., 2002; Fischer and Schott, 2002). Furthermore, tracer calculations using a advective–diffusive model with mean flow and diffusivities derived from float data (Straneo et al., 2003) show transit time distributions that are very broad and asymmetric (and resemble Inverse Gaussian distributions), e.g., Fig. 15 of Pickart et al. (2003).

Broad TTDs imply that mixing plays an important role in transport over decadal time-scales. However, the transit time analysis cannot, alone, distinguish between different possible types of mixing, e.g., whether it is due to diapycnal mixing or isopycnal stirring by eddies. Furthermore, in general it is not possible to quantitatively relate characteristic of TTDs, such as the mean and width, to other diagnostics of mixing, such as isopycnal diffusivities. This is because the width Δ depends on the integrated effect of mixing, whereas diffusivities κ measure local mixing, and there need be no link between Δ and κ locally. One way to compare the different diagnostics is using the relationship that the Peclet number $Pe = (\Gamma/\Delta)^2$, which holds for one-dimensional flows (e.g., Waugh and Hall, 2002). Our result that $\Delta/\Gamma \geq 0.75$ then implies $Pe < 1.8$. This value is

similar to values obtained using previous estimates of isopycnal diffusivities. Several studies have estimated diffusivities of $O(10^7)$ cm^2/s (e.g., Cunningham and Haine, 1995; Khatiwala et al., 2002; Straneo et al., 2003), and combining this value with mean velocities of around 2 cm/s (Lavender et al., 2000) and a length scale of 100 km (typical recirculation scales) yields a Peclet number around 2. (See also Fig. 4 of Straneo et al. (2003) which shows that Pe in the western part of the subpolar gyre is around or less than 3 away from the boundaries, with some regions with Pe less than 1.) Although this comparison shows reasonable agreement it is important to note that the assumed relationship $Pe = (\Gamma/\Delta)^2$ may not hold in general, and further analysis of the relationships between characteristics of TTDs and traditional mixing diagnostics is required. We are currently examining this issue using transport calculations driven by the mean flow and diffusivities derived from float data (as in Straneo et al., 2003).

The fact that there is wide range of transit times needs to be taken into account when interpreting and using transient tracer data. One such application is the estimation of anthropogenic carbon (DIC_{ant}). Using the TTDs inferred from the transient tracer measurements we have estimated DIC_{ant} in the subpolar North Atlantic. The values we obtain are, in most instances, smaller than previous estimates from methods that assume weak mixing. This is true even if only the uptake over the last two decades is considered, in which case use of CFC age as the water mass age overestimates the uptake by 20–30% in most of the subpolar North Atlantic. The uncertainty in our estimates of DIC_{ant} due to the uncertainty in the exact characteristics of the TTDs and CFC age is relatively small (5–10%). There is also uncertainty in the surface DIC_{ant} time series; in particular the assumption of constant disequilibrium. However, allowing variable disequilibrium always acts to reduce DIC_{ant} (Hall et al. (2004) estimate that this reduction is 6–9%, for the Indian Ocean), and so our estimates, which are lower than previous estimates, most likely represent upper bounds on DIC_{ant} .

Another application of TTDs is the interpretation of the propagation of temperature and salinity anomalies in LSW. The time lag in these anomalies has been used to estimate transit times from the Labrador Sea, and, as discussed in the Introduction, these transit times are generally much shorter than CFC ages. This difference in time scales may be due to the existence of a wide range of transit times. For flows with broad TTDs the phase of high frequency variations propagate much faster than that of a slowly changing tracer (Hall and Plumb, 1994; Waugh and Hall, 2002), and so the propagation time of LSW anomalies (in temperature, salinity or CFCs) is expected to be much shorter than CFC ages calculated relative to the slowly increasing atmospheric concentrations. In fact, preliminary calculations using the TTDs determined in this study yield time lags in LSW anomalies that are much smaller than CFC ages and are broadly consistent with observations (e.g., Sy et al., 1997). We are currently performing a more detailed analysis of the propagation of LSW anomalies. This analysis may yield more refined constraints of the TTDs, including information on temporal variations in the transport.

Acknowledgements

We thank Uli Fleischmann for providing us data from the 1994 A1 and A2 cruises, and Scott Doney for the A16 data. We also thank three anonymous reviewers for helpful comments. This work was partially supported by National Science Foundation.

References

- Andrie, C., Jean-Baptiste, P., Merlivat, L., 1988. Tritium and helium 3 in the North Atlantic Ocean during the 1983 TOPOGULF cruise. *Journal of Geophysical Research* 93, 12,511–12,524.
- Beining, P., Roether, W., 1996. Temporal evolution of CFC 11 and CFC 12 concentrations in the ocean interior. *Journal of Geophysical Research* 101, 16,455–16,464.
- Bower, A.S., Le Cann, B., Rossby, T., Zenk, W., Gould, J., Speer, K., Richardson, P.L., Prater, M.D., Zhang, H.M., 2002. Directly measured mid-depth circulation in the northeastern North Atlantic Ocean. *Nature* 419, 603–607.

- Bu, X., Warner, M.J., 1995. Solubility of chlorofluorocarbon 113 in water and seawater. *Deep-Sea Research I* 42, 1151–1161.
- Chen, C.-T., Millero, F.J., 1979. Gradual increase in oceanic CO₂. *Nature* 277, 205.
- Chhikara, R.S., Folks, J.L., 1989. The Inverse Gaussian Distribution: theory, Methodology and Applications. Marcel Dekker, New York.
- Cunningham, S.A., Haine, T.W.N., 1995. On Labrador Sea Water in the Eastern North Atlantic. Part II: mixing dynamics and the advective–diffusive balance. *Journal of Physical Oceanography* 25, 666–678.
- Curry, R.G., McCartney, M.S., Joyce, T.M., 1998. Oceanic transport of subtropical climate signals to mid-depth subtropical waters. *Nature* 391, 575–577.
- Deleersnijder, E., Campin, J., Delhez, E.J.M., 2001. The concept of age in marine modeling I. Theory and preliminary model results. *Journal of Marine Systems* 28, 229–267.
- Doney, S.C., Jenkins, 1988. The effect of boundary-conditions on tracer estimates of thermocline ventilation rates. *Journal of Marine Research* 46, 947–965.
- Doney, S.C., Jenkins, W.J., Bullister, J.L., 1997. A comparison of ocean tracer dating techniques on a meridional section in the eastern North Atlantic. *Deep-Sea Research I* 44, 603–626.
- Fine, R.A., 1995. Tracers, time scales, and the thermohaline circulation: The lower limb in the North Atlantic Ocean. *Reviews of Geophysics Suppl.*, 1353–1365.
- Fine, R.A., Rhein, M., Andrie, C., 2002. Using a CFC effective age to estimate propagation and storage of climate anomalies in the deep Western North Atlantic Ocean. *Geophysical Research Letters* 29(24), 10.1029/2002GL015618.
- Fischer, J., Schott, F., 2002. Labrador Sea Water tracked by profiling floats—From the boundary current into the ocean North Atlantic. *Journal of Physical Oceanography* 32, 573–584.
- Fleischmann, U., Hildebrandt, H., Putzka, A., Bayer, R., 2001. Transport of newly ventilated deep-water from the Iceland Basin to the West European Basin. *Deep-Sea Research I* 48, 1793–1819.
- Gruber, N., 1998. Anthropogenic CO₂ in the Atlantic Ocean. *Global Biogeochemical Cycles* 12, 165–191.
- Gruber, N., Sarmiento, J.L., 2002. Biogeochemical/physical interactions in elemental cycles. In: Robinson, A.R., McCarthy, J.J., Rothschild, B.J. (Eds.), *The Sea: Biological-Physical Interactions in the Oceans*, vol. 12. Wiley, New York, pp. 337–399.
- Gruber, N., Sarmiento, J.L., Stocker, T.F., 1996. An improved method for detecting anthropogenic CO₂ in the oceans. *Global Biogeochemical Cycles* 10, 809–837.
- Haine, T.W.N., Hall, T.M., 2002. A generalized transport theory: water-mass composition and age. *Journal of Physical Oceanography* 32, 1932–1946.
- Haine, T.W.N., Richards, K.J., 1995. The influence of the seasonal mixed-layer on oceanic uptake of CFCs. *Journal of Geophysical Research* 100, 10,727–10,744.
- Hall, T.M., Plumb, R.A., 1994. Age as a diagnostic of stratospheric transport. *Journal of Geophysical Research* 99, 1059–1070.
- Hall, T.M., Haine, T.W.N., Waugh, D.W., 2002. Inferring the concentration of anthropogenic carbon in the ocean from tracers. *Global Biogeochemical Cycles*, 16, 10.1029/2001GB001835.
- Hall, T.M., Waugh, D.W., Haine, T.W.N., Robbins, P.E., Khaliwala, S., 2004. Reduced estimates of anthropogenic carbon in the Indian Ocean due to mixing and time-varying air-sea CO₂ disequilibrium. *Global Biogeochemical Cycles* 18, 10.1029/2003GB002120.
- Huhn, O., Roether, W., Beining, P., Rose, R., 2001. Validity limits of carbon tetrachloride as an ocean tracer. *Deep-Sea Research I* 48, 2025–2049.
- Hunter-Smith, R.J., Balls, P.W., Liss, P.S., 1983. Henry's Law constants and the air-sea exchange of various low molecular weight halocarbon gases. *Tellus B* 35, 170–176.
- Jenkins, W.J., 1988. The use of anthropogenic tritium and helium-3 to study subtropical gyre ventilation and circulation. *Philosophical Transactions of the Royal Society of London Series A* 325, 43–61.
- Jenkins, W.J., Clarke, W.B., 1976. The distribution of ³He in the Western Atlantic Ocean. *Deep-Sea Research* 23, 481–494.
- Khaliwala, S., Visbeck, M., Schlosser, P., 2001. Age tracers in an ocean GCM. *Deep-Sea Research I* 48, 1423–1441.
- Khaliwala, S., Schlosser, P., Visbeck, M., 2002. Rates and mechanisms of water mass transformation in the Labrador Sea as inferred from tracer observations. *Journal of Physical Oceanography* 32, 666–686.
- Koltermann, K.P., Sokov, A.V., Tereschenko, V.P., Bobroli-
bov, S.A., Lorbacher, K., Sy, A., 1999. Decadal changes in the thermohaline circulation of the North Atlantic. *Deep-Sea Research II* 46, 109–138.
- Kortzinger, A., Mintrop, L., Duinker, J.C., 1998. On the penetration of anthropogenic CO₂ into the North Atlantic Ocean. *Journal of Geophysical Research* 103, 18,681–18,689.
- Kortzinger, A., Rhein, M., Mintrop, L., 1999. Anthropogenic CO₂ and CFCs in the North Atlantic Ocean—a comparison of man-made tracers. *Geophysical Research Letters* 26, 2065–2068.
- Lavender, K.L., David, R.E., Owens, W.B., 2000. Mid-depth recirculation observed in the interior Labrador and Irminger Seas by direct velocity measurements. *Nature* 407, 66–69.
- McNeil, B.I., Matear, R.J., Key, R.M., Bullister, J.L., Sarmiento, J.L., 2003. Anthropogenic CO₂ uptake by the ocean based on the global chlorofluorocarbon data set. *Science* 299, 235–239.
- Ostlund, H.G., Rooth, C.G.H., 1990. The North Atlantic tritium and radiocarbon transients 1972–1983. *Journal of Geophysical Research* 95, 20,147–20,165.
- Pickart, R.S., Smethie, W.M., Lazier, J.R.N., Jones, E.P., Jenkins, W.J., 1996. Eddies of newly formed upper Labrador Sea Water. *Journal of Geophysical Research* 101, 20,711–20,726.

- Pickart, R.S., Straneo, F., Moore, G.W.K., 2003. Is Labrador Sea Water formed in the Irminger Basin? *Deep-Sea Research I* 50, 23–52.
- Rhein, M., Fischer, J., Smethie, W.M., Smythe-Wright, D., Weiss, R.F., Mertens, C., Min, D.H., Fleischmann, U., Putzka, A., 2002. Labrador Sea Water: pathways, CFC-inventory and formation rates. *Journal of Physical Oceanography* 32, 648–665.
- Roether, W., Klein, B., Bulsiewicz, K., 2001. Apparent loss of CFC-113 in the upper ocean. *Journal of Geophysical Research* 106, 2679–2688.
- Schlosser, P., Bullister, J.L., Fine, R., Jenkins, W.J., Key, R., Lupton, J., Roether, W., Smethie Jr., W.M., 2001. Transformation and age of water masses, in *Ocean Circulation and Climate*. In: Siedler, G., Church, J., Gould, J. (Eds.), *Ocean Circulation and Climate*. New York, pp. 431–454.
- Seshadri, V., 1999. *The Inverse Gaussian Distribution*. Springer, New York.
- Smethie, W.M., Fine, R.A., Putzka, A., Jones, E.P., 2000. Tracing the flow of North Atlantic Deep Water using chlorofluorocarbons. *Journal of Geophysical Research* 105, 14,297–14,323.
- Straneo, F., Pickart, R.S., Lavender, K., 2003. Spreading of Labrador Sea Water: an advective–diffusive study based on Lagrangian data. *Deep-Sea Research I* 50, 701–719.
- Sy, A., Rhein, M., Lazier, J.R.N., Koltermann, K.P., Meincke, J., Putzka, A., Bersch, M., 1997. Surprising rapid spreading of newly formed intermediate waters across the North Atlantic Ocean. *Nature* 386, 675–679.
- Talley, L.D., McCartney, M.S., 1982. Distribution and circulation of Labrador Sea Water. *Journal of Physical Oceanography* 12, 1189–1205.
- Thomas, H., Ittekkot, V., 2001. Determination of anthropogenic CO₂ in the North Atlantic Ocean using water mass ages and CO₂ equilibrium chemistry. *Journal of Marine Systems* 27, 325–336.
- Thomas, H., England, M.H., Ittekkot, V., 2001. An off-line 3D model of anthropogenic CO₂ uptake by the oceans. *Geophysical Research Letters* 28, 547–550.
- Top, Z., Clarke, W.B., Jenkins, W.J., 1987. Tritium and primordial helium-3 in the North Atlantic: a study in the region of Charlie-Gibbs Fracture Zone. *Deep-Sea Research* 34, 287–298.
- Walker, S.J., Weiss, R.F., Salameh, P.K., 2000. Reconstructed histories of the annual mean atmospheric mole fractions for the halocarbons CFC-11, CFC-12, CFC-113, and carbon tetrachloride. *Journal of Geophysical Research* 105, 14,285–14,296.
- Wallace, D.W.R., 2001. An introduction to special session: ocean measurements and model of carbon sources and sinks. *Global Biogeochemical Cycles* 15, 3–10.
- Wallace, D.W.R., Lazier, J.R.N., 1988. Anthropogenic chlorofluoromethanes in newly formed Labrador sea-water. *Nature* 332, 61–63.
- Wallace, D.W.R., Beining, P., Putzka, A., 1994. Carbon tetrachloride and chlorofluorocarbons in the South Atlantic Ocean, 19°S. *Journal of Geophysical Research* 99, 7803–7819.
- Wanninkhof, R., Doney, S.C., Peng, T.H., Bullister, J.L., Lee, K., Feely, R.A., 1999. Comparison of methods to determine the anthropogenic CO₂ invasion into the Atlantic Ocean. *Tellus B* 51, 511.
- Warner, M.J., Weiss, R.F., 1985. Solubilities of chlorofluorocarbons 11 and 12 in water and seawater. *Deep-Sea Research* 32, 1485–1497.
- Waugh, D.W., Hall, T.M., 2002. Age of stratospheric air: theory, observations, and models. *Reviews of Geophysics* 40(4), 10.1029/2000RG000101.
- Waugh, D.W., Hall, T.M., Haine, T.W.N., 2003. Relationships among Tracer Ages. *Journal of Geophysical Research* 108 (5), 10.1029/2002JC001325.
- Waugh, D.W., Vollmer, M.K., Weiss, R.F., Haine, T.W.N., Hall, T.M., 2002. Transit time distributions in Lake Issyk-Kul. *Geophysical Research Letters* 29(24), 10.1029/2002GL016201.
- Wunsch, C., 2002. Oceanic age and transient tracers: analytical and numerical solutions. *Journal of Geophysical Research* 107, 10.1029/2001JC000797.